R. M. Guedes (Ed.), Creep and fatigue in polymer matrix composites, 2010, Woodhead Pub.

Chapter 2
Time-temperature-age superposition principle and its application to linear viscoelastic materials

E. J. Barbero[1]
Mechanical and Aerospace Engineering, West Virginia University,
Morgantown, WV 26506-6106, USA

List of Figures

1 Compliance of a material described by (5) with $D_0 = 1\,GPa^{-1}, D_1 = 9\,GPa^{-1}$, and two values of the retardation time $\tau = 10\,s$, and $\tau_r = 100\,s$. 16
2 Double logarithmic plot of compliance for the material in Figure 1. 16
3 Momentary curves $D(\lambda)$ at various temperatures, all with age $t_e = 166\,hr$; momentary master curve $D(\lambda; t_e)$ at $T_r = 40^\circ\ C$ (solid line under the shifted data at 40^oC); and shifted to 100^oC (dotted line). 17
4 Approximate time span over which two momentary curves superpose. 18
5 Momentary master curves $D(\lambda)$ at temperatures $T = 40^\circ\ C, 60^\circ\ C, 90^\circ\ C$, all with age $t_e = 1\,hr$, compared to long term data at those same temperatures and ages. The predictions are based on the discussion in Section 4. 18
6 Temperature shift factor plot for the data in Figure 3. $T_r = 40^oC, t_e = 166\ hr$. $C_1 = -1.22503, C_2 = -122.669, C_{1v} = -0.0762931, C_{2v} = -116.057$. 19
7 Compliance vs. time at constant temperature $T = 115^oC$ and various ages. Squares represent data. Circles represent shifted data. Solid lines represent power-law regression of the data. The broken line represents the momentary master curve shifted to $5,000\ hr$. 20
8 Power law model for the creep data in Figure 7 with $\overline{m} = 0.264$ ($T_r = 115^oC, t_{er} = 879\ hr$). 20
9 Ageing shift factor plot for the creep data in Figure 8. The data point on the lower right corner of the figure is the shift factor $a_e = 1$ at $t_{er} = 879\,hr$ ($T_r = 115^oC$). . . . 21
10 Comparison between momentary master curves obtained from temperature and ageing study. The original momentary master curves have been shifted to a common temperature $T = 60^oC$ and age $t_e = 1\ hr$. 21

[1] The final publication is available at www.woodheadpublishing.com Woodhead Publishing ISBN 978-1-84569

List of Tables

1 Regression parameters and shift factors for the TTSP study depicted in Figure 3. . . 22
2 Initial regression parameters for the ageing study depicted in Figure 7. 22
3 Regression parameters and shift factors for the ageing study depicted in Figure 7. . . 22

Abstract

Viscoelastic response such as creep and relaxation are strongly affected by temperature and age for all materials in the range of time when they exhibit viscoelastic effects. Effective time-temperature superposition (ETTSP) is introduced in this chapter to predict long term viscoelastic behavior from short term experimental data. Since the material responds to both temperature and age in the time span of interest, both phenomena are studied, isolated, and described. First, the traditional time-temperature superposition (TTSP) is described and the need to use momentary curves to construct the momentary master curve is addressed. Next, the time-age superposition is described and modeled. Then, the concept of effective time brings everything together into a useful predicting tool. Finally, the methodology is applied to the problem of temperature compensation during long term testing.

Keywords

Ageing, Creep, Effective time, Master curve, Momentary data, Shift factor, Superposition, Temperature compensation, ETT, TTSP

1 Correlation of short-term data

Material characterization provides the information needed to support structural analysis and design. The first step in a materials characterization program is to regress experimental data to model equations in order to represent such data. For this purpose, consider a creep test where a constant stress σ_0 is applied at some time t_e. Denoting by λ the time elapsed since application of the load, the compliance $D(\lambda)$ may be represented by one of a number of possible equations that fit the strain vs. time data. For example, the *standard linear solid* (SLS) model is described by

$$D(\lambda) = D_0 + D_1 \left[1 - e^{-\lambda/\tau}\right] \tag{1}$$

where the retardation time τ is the time it takes for an exponential $e^{-\lambda/\tau}$ to decay to $100 \times e^{-1} = 36.8\%$ of its original value. The larger the τ, the longer it takes for the relaxation modulus $E(\lambda)$ to decay. Since creep tests are easier to perform than relaxation tests, the compliance $D(\lambda)$ is often measured instead of the relaxation modulus. For a linear, unaging material, they are related by

$$E(\lambda) = L^{-1}\left[\frac{1}{s^2 L\left[D(\lambda)\right]}\right] \tag{2}$$

where $L[\,], L^{-1}[\,], s$, denote the Laplace transform, the inverse Laplace transform, and the Laplace variable, respectively [1, chapter 7]. Momentary data (to be defined shortly) can be transformed as in (2) but long term data cannot, because ageing invalidates Boltzmann's superposition principle [1] even if the material is linear (i.e, when the response does not depend on stress).

A schematic of the SLS model using spring and dashpot elements is shown in [1, Figure 7.1.c]. Note that, in the context of linear viscoelasticity (Chapter 1), the compliance is not a function of stress. Additionally, a linear viscoelastic material, for which Boltzmann's superposition applies, must have a constitutive model that is not a function of the absolute time t but rather is a function of the time λ elapsed since application of the load [1, Figure 7.3]. Such material is said to be unaging [1, 2, 3]. However, all polymers age at temperatures below their glass transition temperature T_g. Thus, all the matrix-dominated properties of polymer-matrix composites are subject to aging for in-service temperature conditions [4, 5]. A methodology to deal effectively with the aging problem is presented in sections 3 and 4. Furthermore, the constitutive response of all polymers is a function of temperature. Therefore, a methodology to characterize and model temperature effects is presented in sections 2 and 5.

Equation (1) is a very simple model that may not fit the data well. To obtain a better fit, that is, a better regression between the model equation and the data, more spring-dashpot elements can be added in series, as follows

$$D(\lambda) = D_0 + \sum_{j=1}^{n} D_j \left[1 - e^{-\lambda/\tau_j}\right] \tag{3}$$

When the number of elements is very large, one can replace the summation by an integral and the compliance coefficients D_0, D_j, by a *compliance spectrum* $\Delta(\tau)$ as follows

$$D(\lambda) = \int_0^{\infty} \Delta(\tau) \left[1 - e^{-\lambda/\tau} d\tau\right] \tag{4}$$

While (3) and (4) can fit virtually any material compliance provided a large number of terms is used, the *generalized Kelvin model* is more efficient with only four parameters

$$D(\lambda) = D_0 + D_1' \left[1 - e^{(-\lambda/\tau)^m}\right] \tag{5}$$

In order to reduce the time to complete the material characterization, short term tests are used. In this case, it may be difficult to regress (5) to the data because short term material behavior may be impossible to distinguish from a 3-parameter power law (6). Expanding (5) with a Taylor power series results in

$$\begin{aligned} D(\lambda) &= D_0 + D_1' \left(\lambda/\tau\right)^m \left[1 - (\lambda/\tau)^m + ...\right] \\ D(\lambda) &\approx D_0 + D_1 \lambda^m \end{aligned} \tag{6}$$

where $D_1 = D_1'/\tau$. The power law (6) has the advantage that it becomes a straight line with slope m in a log-log plot, as follows

$$\log\left(D(\lambda) - D_0\right) = \log\ D_1 + m\ \log\lambda \tag{7}$$

and thus it is very easy to regress to data by performing a linear regression in log-log scale. Finally, the Kohlrausch model [3, (10)]

$$D(\lambda) = D_0\, e^{(\lambda/\tau)^m} \tag{8}$$

has been shown to fit the compliance of a broad variety of materials [3, Figure 34]. The parameters D_0, τ, shift the curve in the vertical and horizontal directions, respectively, and the parameter $m \leq 1$ stretches the exponential in time.

Since all the data is manipulated in log-log scale, it is best to sample data uniformly in log time, not uniformly in time. Uniform time-sampling yields data points in log scale that are closely packed for long times. Then, regression algorithms used to fit model equations tend to bias the regression towards longer times. However, most automatic data sampling equipment sample uniformly in time. A simple MATLAB$^{\text{TM}}$ algorithm can be used to pick data uniformly spaced in log time from a set of data uniformly spaced in time [6], as follows

```
% log sampling, user picks the initial time and increment time
% xi(:,1) time (equally spaced in time)
% xi(:,2) compliance
ndp = length(xi(:,1));      %# data points read
tf = xi(ndp,1);             %final time
logti = -1;                 %log of initial time to sample, user choice
del_logti = 0.1;            %log time interval to sample, user choice
logt = [logti:del_logti:log10(tf)]; %equally spaced in log scale
tr = 10.^logt;              %back to time scale
nr = length(tr);            %number of newly sampled data
if tr(nr)~=tf;
    tr = [tr,tf];           %add the final time
    nr = length(tr);        %number of newly sampled data
end
rcount = 1;
for i=1:ndp
    if xi(i,1) >= tr(rcount)        %say 10^-0.1
        xo(rcount,:) = xi(i,:);     %copy data equally spaced in log(time)
        rcount = rcount+1;
    end
    if rcount > nr, break, end;
end
```

2 Time-temperature superposition

In this section, the classical superposition method is described wherein the acceleration factor is temperature. The notion of momentary data is introduced along with a full description of the technique used to obtain the time-temperature momentary master curve and temperature shift factor plot.

To illustrate the principle of superposition, let $D_0 = 1\,GPa^{-1}, D_1 = 9\,GPa^{-1}$, and consider two temperatures[2] $T > T_r$ for which the retardation times (in (9)) are $\tau = 10\,s$ and $\tau_r = 100\,s$, respectively. The compliance vs. time $D(\lambda;T)$ and $D(\lambda;T_r)$, are shown in Figure 1. Note that creep strain develops slower for the larger retardation time. The same curves are shown in double logarithmic scale in Figure 2.

The creep data at temperatures T and T_r are described by SLS models like (1), as follows

$$\begin{aligned} D(\lambda;T) &= D_0 + D_1\left[1 - e^{-\lambda/\tau}\right] \\ D(\lambda;T_r) &= D_{0r} + D_{1r}\left[1 - e^{-\lambda/\tau_r}\right] \end{aligned} \tag{9}$$

If one can shift curve T onto curve T_r (Figure 2) and they superpose nicely, it is said that the curves are superposable.

To shift the curve T horizontally, one plots the creep values $\log D(\lambda;T)$ vs. $\log a_T\lambda$ instead of $\log\lambda$, where $a_T(T)$ is the horizontal shift factor. Since $\log a_T\lambda = \log\lambda + \log a_T$, then $a_T > 1$ shifts the curve T to the right onto the *master curve* T_r, the later having $a_T = 1$ by definition[3]. To shift the curve T vertically, one divides the values of $D(\lambda;T)$ by a vertical shift factor $b(T)$. If the curves are superposable, $D(\lambda;T)$ at time λ is equal to $b_T D(a_T\lambda;T_r)$ at time $a_T\lambda$ (see Figure 1). Mathematically,

$$D(\lambda;T) = b_T D(a_T\lambda;T_r) \tag{10}$$

For this simple example, $D_0 = D_{0r}$ and $D_1 = D_{1r}$; that is, the only difference between them are the retardation times τ, τ_r. Then, $b_T = 1$ and using (9)

$$D_0 + D_1\left[1 - e^{-\lambda/\tau}\right] = D_0 + D_1\left[1 - e^{-a_T\lambda/\tau_r}\right] \tag{11}$$

from which

$$\tau = \tau_r/a_T \tag{12}$$

Since $a_T > 1$, then $\tau < \tau_r$. Therefore, the well known fact that creep strain grows faster at

[2] or two ages $t_e < t_{e,r}$

[3] Note that the entire formulation could be done by proposing a shift of the form $\log\lambda/a_T$ instead of $\log aT\lambda$. The two formulations can be easily reconciled noting that the shift factor in one is the reciprocal of the same factor in the other.

temperature $T > T_r$ is described by a shorter retardation time $\tau < \tau_r$.

Since creep strain grows faster at temperature $T > T_r$, one can accelerate a test by running it at a higher temperature, within limits so that the material does not degrade. In this case the retardation times at temperature T are reduced by a factor $1/a_T$ (see (12)) and creep is accelerated by a factor a_T. This is the basis of widely used *accelerated testing*, but in performing accelerated testing, one must be careful that the acceleration factor (temperature in this case) does not affect the physical or chemical characteristics of the material.

For ageing, the well known fact that age stiffens polymers is described by a retardation time $\tau < \tau_r$ when $t_e < t_{er}$, with t_e being the aging time, or simply age, of the material and t_{er} being another age taken as reference. In this case the ageing shift factor is denoted as a_e. If the momentary compliance $D(\lambda; t_e)$ of a specimen with age t_e is plotted vs. time $a_e\lambda$, it superposes the compliance of a specimen with age t_{er}. Aging time t_e is the time elapsed since the sample was quenched.

In principle, the data obtained at higher temperature can be shifted to lower temperature in order to predict the creep compliance at lower temperature for times that exceed the time available to do the test. However, no other physical or chemical phenomena should interfere with the superpositions being made. If the material ages during the test, the data will not superpose [7, 8].

To solve this problem, the individual tests must be of duration short enough that the effects of aging are negligible. This is accomplished by restricting the time of the tests to $\lambda/t_e < 1/10$, where λ is the time of the test started at age t_e. This is called *snapshot condition* and the individual curves thus obtained are called *momentary* curves [3]. The effective time λ is used to describe momentary data in order to distinguish it from the real time t. The total time since the sample was quenched is $t_e + \lambda$. The concept of effective time is formalized in section 3. For now it suffices to say that λ is time elapsed since the application of the load and with no further ageing, which is accomplished by testing for short times, within the snapshot condition $\lambda/t_e < 1/10$.

To obtain the temperature shift factors a_T, b_T, a number of experiments are performed at increasingly higher temperatures in such a way that successive momentary curves superpose when shifted vertically and horizontally. This is illustrated in Figure 3 using data from [4].

The objective of superposing data sets is to construct a master curve that spans longer time than the time span of each data set. In Figure 3, all data sets span approximately the same time, from 60 s to about 16 hr. The chosen reference temperature is $T_r = 40^oC$. By performing horizontal shifts of magnitude log $a_T(T)$ on the data sets with $T > T_r$, the 16 hr-tail of the curves extend the master curve further and further to the right in log λ scale. Vertical shifts are necessary to obtain the best possible superposition among data sets but horizontal shifts are solely responsible for extending the time span of the master curve. Both horizontal and vertical shifts are necessary to produce the momentary master curve in Figure 3. If vertical shifts were enough to superpose the curves, the resulting master curve would span the same time interval of the original data sets and the objective of time-temperature superposition would not be achieved. Since the data sets (or the curves representing the data sets) are shifted horizontally to the right, they superpose over a time span shorter than the individual curves. Estimating the time span over which the curves superpose is critical for implementing an accurate algorithm to superpose the curves, i.e., to calculate values of a_T, b_T, that yield the best superposition possible. This is illustrated in (Figure 4). Assuming horizontal shift only, the solid-line portion curve at temperature T superposes on the solid-line portion of the curve at temperature T_r when the T-curve is shifted to the right by plotting the compliance $D(a_T\lambda; T)$ vs. time $a_T\lambda$. Therefore the overlapping time-span starts at $\lambda = \lambda_0$ and

ends at $\lambda = \lambda_f/a_T$ (see (10)).

In Figure 3, the compliance $D(\lambda)$ represents the shear compliance S_{66} of a unidirectional (UD) composite lamina, consisting of Derakane 470-36 Vinyl Ester polymer reinforced with 30% by volume of E-glass fibers in a $[45^o]$ UD lamina configuration. A typical experimental setup for larger specimens is presented in [9]. In Figure 3, individual data sets are regressed with the power law model (7) and the coefficients are given in Table 1.

If the momentary data can be fitted exactly with a model equation, such as (1–8), one can fit each curve with a model, then shift the model curves [10], instead of shifting actual data. Such an approach is computationally simpler but, if the model does no fit the data exactly, the shift factor for the models might not yield a smooth master curve when used to shift the actual data. Model equations are regressed based on the average error between the model and the data, and are prone to yield the largest error at the ends of the data interval, precisely where the curves must be superposed. Therefore, the regression errors may be magnified and accumulated in the shift process.

The computer code for determining the temperature shift factors is based on (10). First, the time span where the curves would superpose is approximated (Figure 4) as the interval $[\lambda_0, \lambda_f/a_T]$, where λ_0, λ_f, are the initial and final time of the momentary curve being shifted. Note that while constructing the momentary master curve, specimens are tested at different temperatures but all are aged equally, thus the data for all specimens span approximately the same testing time $[\lambda_0, \lambda_f]$, with $\lambda_f \leq t_e/10$. Then, the value of of the shift factors a_T, b_T, are found by minimizing the norm of the error between the two data sets being superposed. For example, a least squares minimization of the error is implemented by writing (10) as

$$err = \frac{1}{n}\sum_{i}^{n}\left[D(\lambda_i;T) - b_T D(a_T\lambda_i;T_r)\right]^2 \tag{13}$$

where n is the number of data points. Then, the shift factors a_T, b_T are found by minimizing the error [6]. For example, in MATLAB

```
z = fminsearch(@(z)err(@power,ti,tf,beta(k),beta(k-1),z),z0,options);
```

yields the array `z` containing the horizontal and vertical shift factors that minimize the error computed in the function `err`. Further, `@power` is a function fitting the data sets, in this case with (6), with parameters D_0, D_1, m, passed through the array `beta` for temperatures `k` and `k-1`. Finally, `z0` is an initial guess for the array `z` [6].

The shift process produces a momentary master curve $D(\lambda; T_r, t_e)$ for a particular age and temperature t_e, T_r, such as the one shown in Figure 3, that spans much more time λ than that devoted to individual tests. However, this momentary master curve does not include the effect of further aging, because it is made up of momentary curves, and all of them tested at the same age t_e, with each of them experiencing negligible aging during testing for a time span shorter than $t_e/10$. The corollary is that the momentary master curve obtained cannot be used to predict long term creep without further treatment. In fact, the shape of this momentary master curve is very different to that of long term creep, as shown in Figure 5.

The shape of the momentary master curve would predict creep to occur much faster than in reality. As long as ageing produces changes of stiffness in the material, time-temperature super-

position (TTSP) alone cannot predict long term creep. In fact, TTSP alone can only predict long term behavior near the glass transition temperature T_g because aging effects become negligible near the glass transition in a relatively short period of time [3, 11, 12].

Note that $D(\lambda; T_r, t_e)$ refers to the collection of shifted data in Figure 3. It is not necessary to fit such data with a model equation in order to proceed with the discussion. If a model equation is desired for convenience, the analyst is responsible for assuring that the model equation fits the momentary master curve accurately. Further, the momentary master curve $D(\lambda; T_r, t_e)$ can be shifted to any temperature T and age t_e by using the temperature shift factors $a_T(T), b_T(T)$ and ageing shift factor $a_e(t_e)$, respectively (see section 3), i.e.,

$$D(\lambda; T, t_e) = b_T D(a_T\, a_e\, \lambda; T_r, t_{er}) \tag{14}$$

Having performed a series of momentary tests at increasing temperatures, one can plot the shift factor vs. temperature, as shown in Figure 6. A regression using the Williams-Landel-Ferry (WLF) equation

$$\log a_T = \frac{C_1\,(T - T_r)}{C_2 + T - T_r} \tag{15}$$

fits the values of $\log a_T$ vs. T very well, yielding parameters C_1, C_2. The same applies to the vertical shift factor b_T. Note that $C_1 < 0, C_2 < 0$ in Figure 6. Values of C_1, C_2, obtained from data at or above the glass transition temperature T_g are different and cannot be used below T_g [4]. Any abrupt change in the shift factor plot provides an indication of a sudden change in physical or chemical properties such as thermal degradation, phase changes, and so on. The shift factor for any temperature can be predicted from Figure 6 using (15), even for temperatures for which no test data is available. That means that the momentary master curve can be shifted to any temperature. For example, the momentary master curve for temperature $T = 100^oC$, for which no experimental data is available, is shown in Figure 3 (dotted line).

Usually, a SLS model (1) does not fit creep data satisfactorily, so more terms need to be used (see (3)). Then, a necessary condition for the curves to be superposable is that all the retardation times τ_j shift equally by a single shift factor a_T. Phenomenologically, this means that all the physical processes described by those many retardation times must change equally with temperature, or whatever phenomenon is being studied (i.e., age, stress, etc.), for superposition to be feasible.

If the data is represented by a compliance spectrum like in (4), then, using the same reasoning described above, (10) yields

$$\Delta(\tau; T) = a_T \Delta(a_T\ \tau; T_r) \tag{16}$$

that is, the whole compliance (or retardation) spectrum must be affected equally by a scalar shift factor in order for superposition to apply. The method presented in this section is called time-temperature superposition *principle* because it has not been derived from some underlying principle, but rather it is a principle itself, which is valid only as long as the curves are superposable.

3 Time-age superposition

In this section, the characterization of aging is described by a technique similar to that of section 2. Since the momentary (unaged) master curve has been obtained already (Figure 3) by time-temperature superposition, constructing an aging-time master curve is only necessary as an intermediate step for obtaining the ageing shift factor μ_e, which is defined in (22) and allows for the calculation of the ageing shift factor a_e for any age t_e. In summary, ageing can be characterized by just one scalar value, μ_e, which is the slope of $\log a_e$ vs. $\log t_e$.

Physical ageing begins when the polymer is quenched to a temperature below T_g, wether the material is under load or not. Annealing of the material slightly above T_g erases all the memory in the material; thus, the material is rejuvenated [3]. Quenching to a temperature well below T_g starts the age clock for the material.

In order to elucidate the effects of ageing, a series of creep tests are performed at various ages. At each age t_e, a creep test is conducted for a time λ no longer than $t_e/10$ so that the creep compliance obtained is not tainted by the effect of ageing. This is a momentary curve obtained while satisfying the snapshot condition. To improve the quality of the regression, the ages at which creep testing takes place are chosen to be approximately equidistant on a log scale. This is easily accomplished by testing at 0.1, 0.3162, 1., 3.1623, 10., units of time, and so on (MATLAB: `10.^([-1:.5:1])`). Compliance vs. time curves in double-logarithmic scale are shown in Figure 7 and Table 3; the solid lines are obtained regressing the data with the power law model (6). It can be seen that the regression is excellent.

For long ageing time, the testing time can be relative long and thus complex equations, such as (5), may be fitted to the data. However, one is interested in elucidating the effects of ageing with as short time testing as possible. This leads to short ageing times and even shorter creep testing times. For short times, there is not enough data to elucidate the many parameters involved in say, a four-parameter model (5). Therefore, a simpler model is required, such as the power law (6), re-written as follows

$$D_c(\lambda) = D(\lambda) - D_0 = D_1 \lambda^m \tag{17}$$

where D_c is the creep compliance, D_0 is the elastic compliance, and $D(\lambda)$ is the total compliance measured in the experiment.

Each data set is initially regressed to the power law model (6) to determine D_0, D_1, m. Numerical results are shown in Table 2. Assuming that the elastic compliance is independent of age, D_0 should be the same for all data sets. This is confirmed by the low coefficient of variance (COV) for D_0 in Tables 2 and 3. Similarly, in [13, 14], no correlation was observed between initial compliance D_0 and age t_e. Small variations of D_0 are due to small inaccuracies in the test, such as compliance of the equipment, imperfect initial contact between specimens and loading points, etc. For this reason, the data from the first two tests on each specimen were discarded in [13, 14], recognizing the need for mechanical conditioning of the specimens.

The resulting power law exponent m might not identical for all plots, i.e., for all ages, but the dispersion usually is very small. For example, for the data in Figure 7, the average is $\overline{m} = 0.228$ with a COV=16.8%. If the first test (at $t_e = 2\ hr$) is neglected, as recommended in [13, 14], the COV reduces to COV=7%. The remaining dispersion is caused by the variable amount of data

(spanning $(t_0, t_e/10)$) available to perform the correlation for various ages, with tests at long ages having the most data points.

Then, the data is regressed again with (17), but this time keeping $m = \overline{m}$ constant for all curves and adjusting only D_0, D_1. Numerical results are shown in Table 3. As it can be seen in Figure 8, the impact of such averaging is minimal [9]; i.e., the model still regresses the data very well.

With all the curves having the same power-law exponent, they are parallel lines in a plot of $\log(D - D_0)$ vs. $\log\ t$ as shown in Figure 8. Then, the log of the shift factor, $\log a_e$, can be measured as the horizontal distance between any given curve and the master curve in the same figure. Noting that the creep compliances are represented by parallel lines, they are obviously superposable. Mathematically, to say that creep compliances are superposable means that

$$D_c(\lambda; t_e) = D_c(a_e\lambda; t_{er}) \tag{18}$$

where $D_c(\lambda; t_{er})$ is the creep compliance of the reference curve for the reference age t_{er}. Writing the log of the power law model for the two sets of data

$$\log D_c(\lambda; t_{er}) = \log D_{1r} + \overline{m}\log(a_e\lambda) \tag{19}$$
$$\log D_c(\lambda; t_e) = \log D_1 + \overline{m}\log(\lambda) \tag{20}$$

and subtracting the second from the first equation yields explicit formulas for the ageing shift factors

$$a_e = \left(\frac{D_1}{D_{1r}}\right)^{1/\overline{m}}$$
$$b_e = D_{0r} - D_0 \tag{21}$$

where $D_{0r}, D_{1r}, \overline{m}$, are the power law model parameters for the reference curve at age t_{er} and $D_0, D_1, \overline{m}$, are the parameters for the curve at age t_e.

To superpose the data sets in a plot of $\log(D - D_0)$ vs. $\log\ t$ as shown in Figure 8, each data set is shifted to the left by $\log a_e$. To superpose them on a plot of $\log\ D$ vs. $\log\ t$ as shown in Figure 7, one need to plot $b_e + D(a_e\lambda)$ vs. $a_e\lambda$ on double logarithmic scale. Note that the factor b_e is not used in the same way as the shift factor b_T. While b_e is added to $D(a_e\lambda)$, $\log\ b_T$ is added to $\log\ D(a_T\lambda)$. This complication is not relevant because the master curve obtained from the ageing study is seldom used; instead the master curve from the temperature study is used. Furthermore, different treatment of vertical shift allowed us to derive a pair of simple formulas, i.e., (21), for the horizontal and vertical ageing shift factors, whereas the temperature shift factors are computed by a numerical minimization algorithm, that is, in an approximate way. The procedure described in this section, concluding into (21), cannot be used to calculate the temperature shift factors in section 2, because creep compliance curves obtained at different temperatures have markedly different values of D_0 (see Table 1).

In this process, it is best to choose the master curve to be the one corresponding to the longest age tested because it is the curve with more data. Also, each specimen is annealed, quenched,

and tested for increasingly longer aging time without removing it from the testing equipment, such as a Dynamic Mechanical Analyzer (DMA) [13]. This means that the data for the longest age is perhaps the best in terms of mechanical conditioning of the sample.

Next, (21) is used to obtain the ageing shift factors a_e for each data set. A linear regression of $-\log\ a_e$ vs. $\log\ t_e$ fits the values very well (Figure 9), and the slope is the aging shift factor rate

$$\mu_e = -\frac{d\log a_e}{d\log t_e} > 0 \tag{22}$$

which is normally assumed to be constant for a wide range of temperatures, except near the glass transition [3, 12]. Temperature dependence was reported in [4, Figure 9].

Once the aging shift factor rate μ_e has been determined, the *ageing* momentary master curve constructed at a given reference age (say $t_{er} = 879\,hr$ in Figure 7) can be shifted to any other age by shifting it to $\log(\lambda/a_e)$, where the aging shift factor is computed from Figure 9 and (22) as

$$\log a_e = -\mu_e \log(t_e/t_{er}) \tag{23}$$

Equation (23) is analogous to the WLF equation (15). For example, the aging momentary master curve for age $t_e = 5,000\,hr$, for which no experimental data is available, is shown in Figure 7 (broken line). Note that shifting to the right of the last data set assumes that the shift factor plot can be extrapolated outside the range of ages for which data is available (2 to 879 hr in this case).

Unlike the case of TTSP (Figure 3), the objective in this section is not to generate a master curve to span longer time than available for experimentation, but to obtain the ageing shift factor plot and from it to calculate the aging shift factor rate μ_e. All the effect of physical ageing is characterized by the aging shift factor rate μ_e. Still, an ageing momentary master curve is produced (Figure 7), which is valid only for the time span up to $t_{er}/10$. Since the power-law model fits the data very well, the ageing momentary master curve is represented by (17) with $D_0, D_1, \overline{m}$, being materials properties determined by the procedure presented in this section. Also, since power-law models fit the master curve in Figures 3 and 7, an argument can be made to extrapolate the longest momentary curve of an ageing study beyond $t_{er}/10$. Such argument has no empirical basis because on a real experiment, aging will mar the data if the testing time goes beyond $t_{er}/10$. Furthermore, lacking a temperature study, one would not know how to apply the momentary curve to any temperature other than that used to conduct the ageing study.

A comparison between momentary master curves obtained from temperature and ageing studies is presented in Figure 10. The original momentary master curves have been shifted to a common temperature $T = 60^oC$ and age $t_e = 1\ hr$. To facilitate comparison, a small, additional vertical shift of $\log\ 1.04\ [1/GPa]$ has been applied to the ETT master curve. The curves are close but not identical. The difference may be attributed to experimental errors. These errors need to be minimized in order to predict long term creep because minor changes in the momentary curve produce large discrepancies in the predicted compliance at long times. For this reason, several replicates should be used to construct the momentary curves, which allows for determination of the mean and variance of the response [13].

In Figure 10, the momentary curve from the temperature study is to the right of the target age

and temperature (i.e., $t_e = 1\ hr, T = 60^oC$). Therefore, it is shifted from $t_e = 166\ hr, T_r = 40^oC$ to $t_e = 1\ hr, T = 60^oC$ by plotting $b_T\ D(\lambda)$ vs. $\frac{1}{a_T a_e}\lambda$ with $a_T = 1.732$, $b_T = 1.037$, and $a_e = 56.306$. The momentary curve from the ageing study is to the right of the target age but to the left of the target temperature. Therefore, it is shifted from $t_e = 879\ hr, T_r = 115^oC$ to $t_e = 1\ hr, T = 60^oC$ by plotting $b_T\ D(\lambda)$ vs. $\frac{a_T}{a_e}\lambda$ with $a_T = 57.057$, $b_T = 1.345$, and $a_e = 209.573$.

4 Effective Time Theory

In this section, the relationship between un-aged and real time, i.e., the concept of effective time is described and used to correct the momentary master curve (Figure 3) for aging, thus proving a methodology for predicting long-term creep.

Effective time theory (ETT) was proposed by Struik in [3]. Considering a test started at age t_e, running for time t, so that the total time since quench is $t_e + t$, from (22), we can calculate the ageing shift factors at times t_e and $t_e + t$ as

$$\begin{aligned} -d\log a_e(t_e) &= \mu_e\, d\log t_e \\ -d\log a_e(t_e + t) &= \mu_e\, d\log(t_e + t) \end{aligned} \tag{24}$$

Therefore, the shift factor evolves with time as

$$a_e(t) = \frac{a_e(t_e + t)}{a_e(t_e)} = \left(\frac{t_e}{t_e + t}\right)^{\mu_e} < 1 \tag{25}$$

On the momentary master curve of the time-age superposition study reported in Figure 7, one may assume that ageing has stopped at $t_e = 879\,hr$ because the testing time is so short (less than $t_e/10$) that no further ageing is allowed to manifest itself. Superposition of momentary compliance curves obtained for increasing ages t_e indicates that the retardation times τ, which represent material behavior, are longer as the sample ages. For $t \to \infty$, ageing stops, and choosing that long age as the reference state to construct the master curve, one has $a_e(\infty) = 1$. Any shorter age has a shift factor $a_e > 1$ because the curves have to be shifted right onto the master curve. At any shorter age, creep accumulates faster with smaller retardation times; the acceleration being $1/a_e$. Therefore, the same amount of creep accumulates in a shorter real time interval dt than in *effective* (ageless) time interval $d\lambda$, which are related by

$$dt = (1/a_e)\, d\lambda \tag{26}$$

which leads to the definition of the *effective time* [3, (85)]

$$\lambda = \int_0^t a_e(\xi) d\xi \tag{27}$$

Substituting (25) and integrating, yields [3, (117-188)]

$$\lambda(t) = t_e \ln\left[1 + t/t_e\right] \qquad \text{if} \quad \mu = 1 \tag{28}$$

$$\lambda(t) = \frac{t_e}{1-\mu}\left[(1 + t/t_e)^{(1-\mu)} - 1\right] \qquad \text{if} \quad \mu < 1 \tag{29}$$

where ln denotes the natural logarithm (base e.)

If the material did not age, the momentary master curve $D(\lambda; t_e)$ on Figure 3 would predict the compliance as a function of time. But since the material does age, the long-term creep compliance $D(t)$ must be smaller, that is

$$D(t) = D(\lambda(t); t_e) \tag{30}$$

with $\lambda(t)$ given by (28,29). The predicted long-term compliance is shown with a solid line in Figure 5. The methodology has been show to provide good predictions of actual long-term creep data [4, Figs. 14-15] and [15].

If the material did not age ($\mu = 0$), the time t and effective time λ would be the same. But the material does age, so $0 < \mu \leq 1$ and the effective time is much shorter than the real time. From (28,29), the real time can be calculated as

$$t/t_e = -1 + \exp(\lambda/t_e) \qquad \text{for } \mu = 1 \tag{31}$$

$$t/t_e = -1 + (\alpha\lambda/t_e + 1)^{1/\alpha} \qquad \text{for } \mu < 1 \tag{32}$$

where $\alpha = 1 - \mu$.

The longest data in the momentary master curve of an aging study, such as Figure 7, is constructed for $\lambda/t_e = 0.1$. According to (31), no prediction can be made for time exceeding $t/t_e = 0.1$, that is $t = 879\,hr$ in the example at hand. The model equation that fits the data cannot be extended beyond $\lambda/t_e = 0.1$ because it is known that as the material ages, the creep rate slows down and the model equation will not fit the data well. Shifting the master curve from say $t_e = 879\,hr$ down to shorter aging time, say $t_e = 30\,min$, does not help predicting long-term creep because approximately the same λ/t_e time span will be covered, up to $\lambda/t_e = 0.1$. Shifting to the right, assuming that the extrapolation of the shift factor plot is valid outside the range for which data is available, does not help to extend the range of the predictions to long times because the momentary curves do not shift much to the right. For example, the shift to $5,000\ hr$ is shown in Figure 7.

In order to predict long-term creep, a momentary master curve that extends beyond $\lambda/t_e = 0.1$ is needed. The momentary master curve from the TTSP study (section 2, Figure 3) serves the purpose [3]. Another option is to shift the momentary curve in Figure 7 to a lower temperature, but for that one needs the temperature shift factor plot form the TTSP study. In that case, a momentary master curve is available with a long time span, such as in Figure 3. Therefore, we shall use the latter.

The time span needed on the momentary master curve (Figure 3) can be calculated easily. For example, if the momentary master curve were constructed with momentary data for $t_e = 166\,hr$, and predictions are sought up to one year, then $t/t_e = 8640/166 = 52$. Assuming the aging study

(section 3) yields $\mu_e \approx 1$, using (31) yields $\lambda/t_e = \ln(t/t_e - 1) = 3.931$, or $\lambda = 652\ hr$. It is not possible to produce experimentally a momentary curve for 652 hours with a material that has been aged for only 166 hours. However, the momentary master curve for $T = 40^oC$ (Figure 3) easily exceeds the 652 hr ($5.6\ 10^6\ s$) required.

Usually, aging studies are conducted at temperatures above room temperature because the test equipment, such as DMA, can hold temperature more stably above (or below) room temperature. As long as there is heat exchange with the environment, the control system of the instrument can hold the temperature accurately. On the contrary, room temperature control relies on the heating, ventilation, and air conditioning (HVAC) system of the building, which is not nearly as accurate as the control system of a dedicated instrument, such as a DMA [13] or environmental chamber [9, 14].

4.1 Summary

The procedure used to predict long-term creep is as follows:

1. Perform a number of creep tests at increasing temperatures for a duration λ not to exceed the snapshot condition $\lambda/t_e < 1/10$. All tests are to be performed with materials aged the same amount, i.e., t_e.

2. Shift the data onto a momentary master curve (Figure 3) by determining the temperature shift factors a_T, b_T, for each temperature. Construct the shift factor plot (Figure 6) and fit it with (15). The resulting momentary master curve represents the momentary compliance $D_{te}(\lambda)$ of the material at age t_e without the effects of any further ageing. Since the temperature shift factors a_T, b_T, can be calculated at any temperature in terms of C_1, C_2, C_{1v}, C_{2v}, the master curve predicts the unaging compliance at any temperature.

3. Perform a number of creep tests at increasing ages for a duration λ not to exceed the snapshot condition $\lambda/t_e < 1/10$. All tests are to be performed at the same temperature, usually at room temperature for convenience.

4. Shift the data onto a master curve by determining the aging shift factor a_e for each age. Construct the shift factor plot $-\log a_e$ vs. $\log t_e$. Compute the ageing shift factor μ_e as the slope of the plot.

5. The long-term compliance is given by (30) with λ given by (28,29) in terms of the real time t.

5 Temperature compensation

In this section, effective time-temperature superposition (ETTSP, described in this sections 2-4) is used to perform temperature compensation of long term data collected in a fluctuating temperature environment.

Field testing of polymer and polymer composite structures, as well as laboratory testing of large structures, are subject to temperature variations due to seasonal and daily temperature fluctuations. Due to temperature fluctuations, the material undergoes changes of creep compliance

and those are reflected in the data collected, particularly in strain readings [15]. Therefore, the data needs to be compensated to report the behavior of the material at a constant temperature T_R. Temperature compensation is not possible by using the time-temperature momentary master curve and temperature shift factor of section 2 because those curves represent the material behavior without aging, as it was at the age t_e used to collect the data in section 2. Obviously, the material undergoes further aging during a long-term test. Furthermore, the field test starts with the material having an age t_R that represents the time between the material was produced and the onset of the field test and it is unlikely that t_R coincides with t_e.

The temperature compensation procedure is as follows. First, the time-temperature momentary master curve $D(\lambda; t_e)$ is shifted to the reference temperature T_R and age t_R by using (15,23) in terms of the known coefficients $\mu_e, C_1, C_2, C_{1v}, C_{2v}$.

Next, each time interval $\Delta t = t_i - t_{i-1}$ of a long term test occurs at a time t_i for which the recorded temperature is $T(t_i)$. The time t_i is shifted to effective time. That is, using (28,29), compute λ_i, λ_{i-1}, and the unaged time interval $\Delta\lambda_i = \lambda_i - \lambda_{i-1}$. This interval can be adjusted to the reference temperature as

$$\Delta\lambda_i' = \Delta\lambda_i / a_T \tag{33}$$

Then, the accumulated aging time at time t_n is computed as

$$\lambda_n' = \sum_{i=1}^{n} \Delta\lambda_i' \tag{34}$$

which is then transformed to real time using (31,32).

6 Conclusions

Age and temperature affect the creep compliance of polymers in similar yet separate ways. Physical ageing changes the material behavior with time, thus invalidating the use of time-temperature superposition for any significant length of time, for any temperature except in the vicinity of the glass transition. As a result of ageing, the material properties change with time and Boltzmann's superposition principle does not longer applies. Combined use of a time-temperature superposition study, performed for a time span short enough to render aging negligible, and an age-time superposition study, enables us to predict the combined effects of temperature and age. The methodology also allows us to recover Boltzmann's superposition principle and thus a plethora of useful analysis techniques based on it, such as prediction of viscoelastic properties of composites [16, 17], and so on. Application of this methodology for the case of stress induced non-linearity awaits attention.

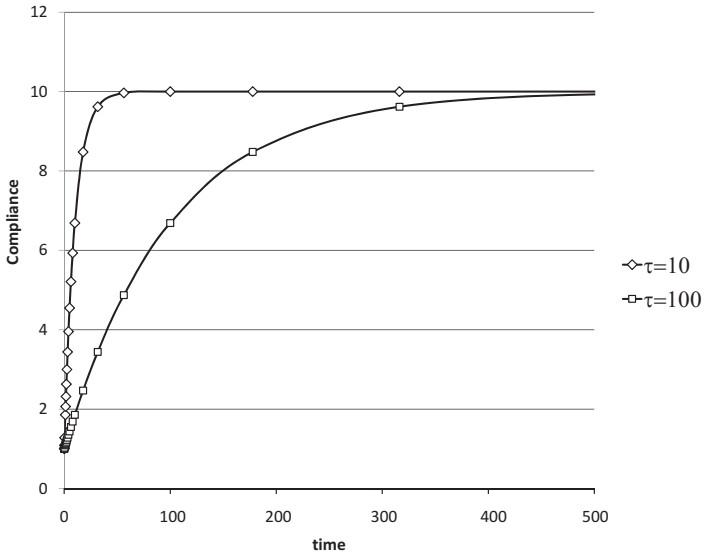

Figure 1: Compliance of a material described by (5) with $D_0 = 1\,GPa^{-1}, D_1 = 9\,GPa^{-1}$, and two values of the retardation time $\tau = 10\,s$, and $\tau_r = 100\,s$.

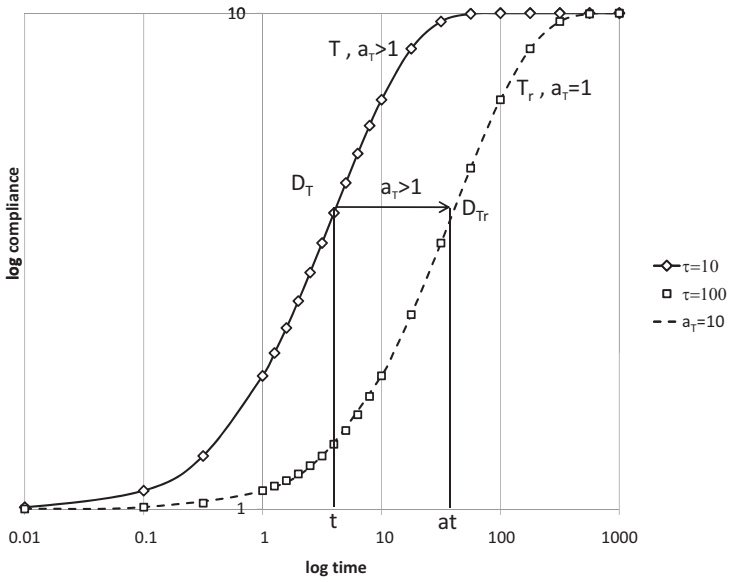

Figure 2: Double logarithmic plot of compliance for the material in Figure 1.

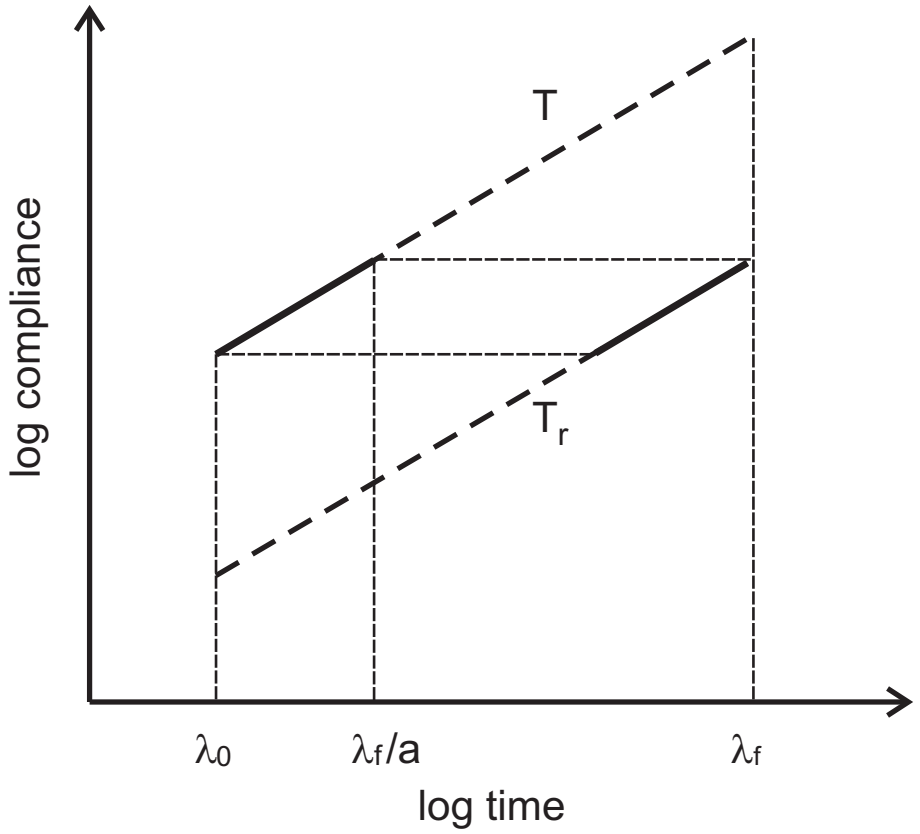

Figure 3: Momentary curves $D(\lambda)$ at various temperatures, all with age $t_e = 166\,hr$; momentary master curve $D(\lambda; t_e)$ at $T_r = 40^\circ\ C$ (solid line under the shifted data at 40^oC); and shifted to 100^oC (dotted line).

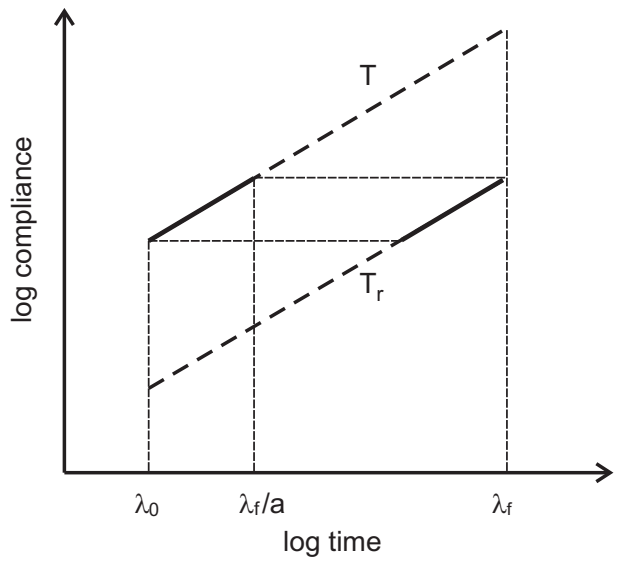

Figure 4: Approximate time span over which two momentary curves superpose.

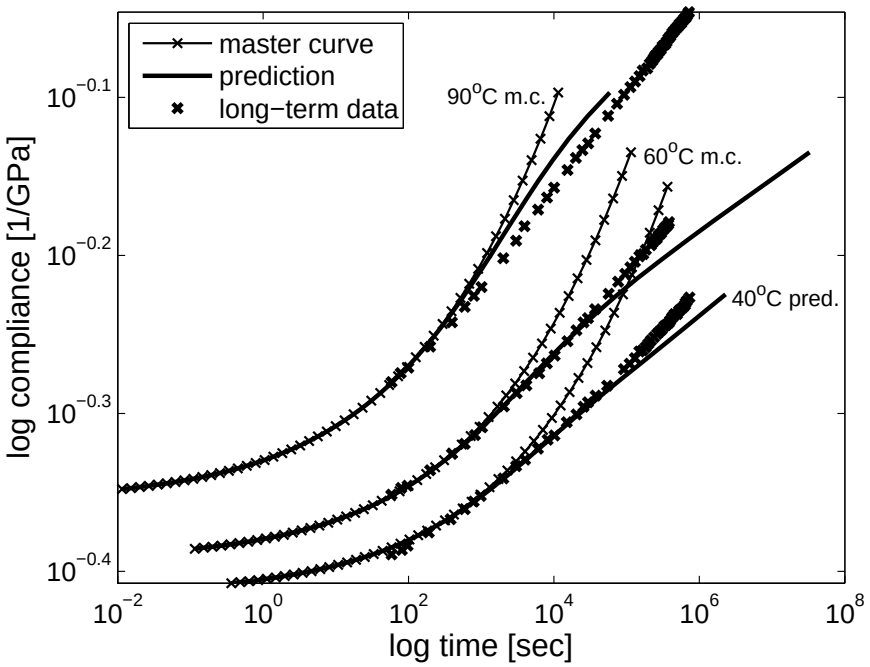

Figure 5: Momentary master curves $D(\lambda)$ at temperatures $T = 40^\circ\ C, 60^\circ\ C, 90^\circ\ C$, all with age $t_e = 1\,hr$, compared to long term data at those same temperatures and ages. The predictions are based on the discussion in Section 4.

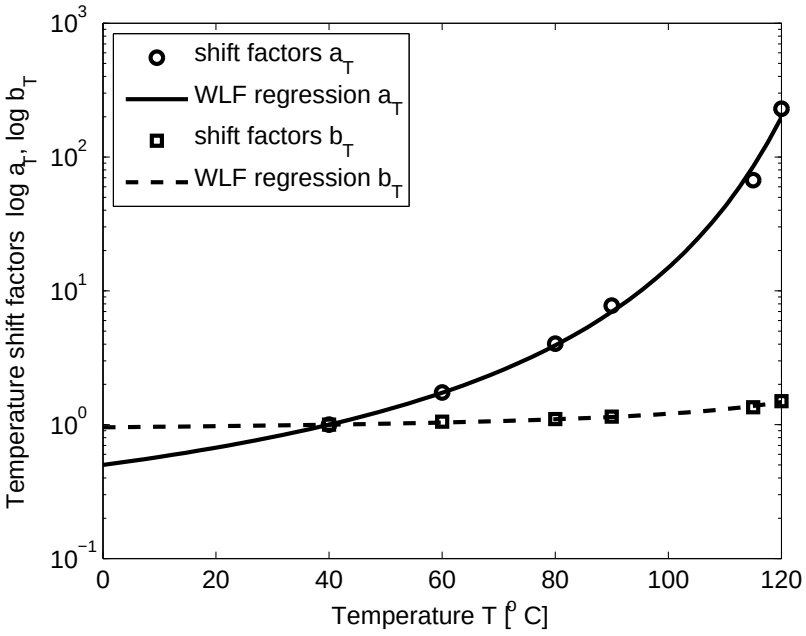

Figure 6: Temperature shift factor plot for the data in Figure 3. $T_r = 40^oC, t_e = 166\ hr$. $C_1 = -1.22503, C_2 = -122.669, C_{1v} = -0.0762931, C_{2v} = -116.057$.

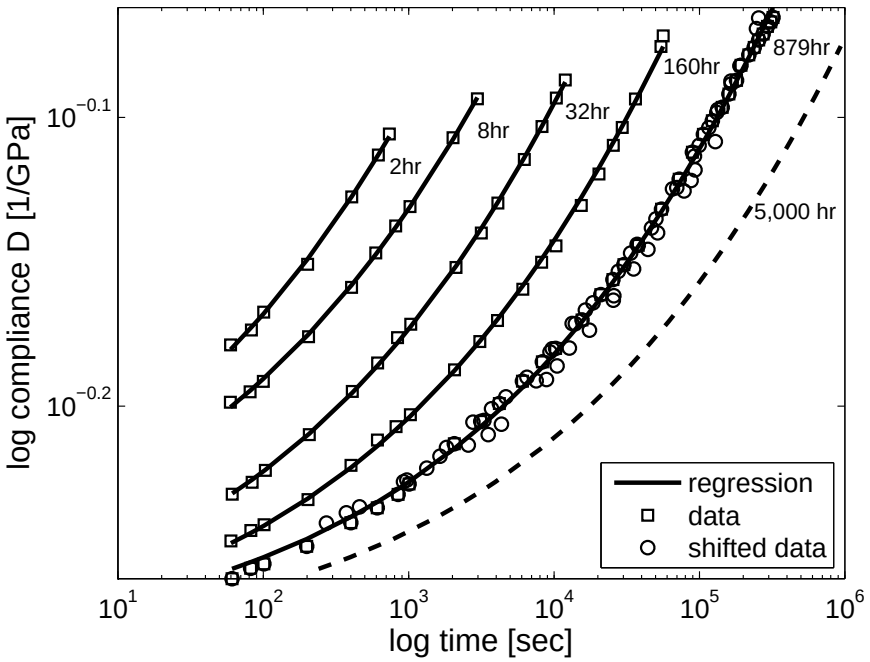

Figure 7: Compliance vs. time at constant temperature $T = 115^oC$ and various ages. Squares represent data. Circles represent shifted data. Solid lines represent power-law regression of the data. The broken line represents the momentary master curve shifted to $5,000\ hr$.

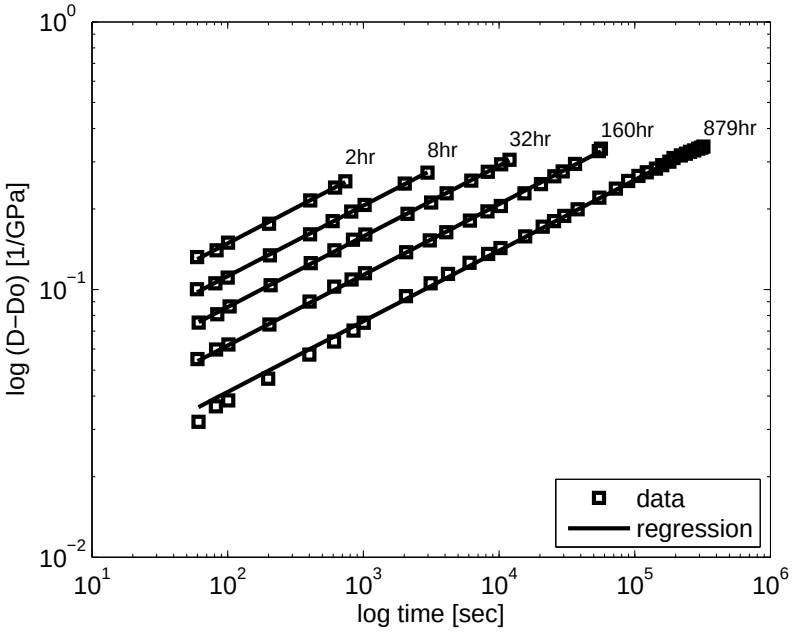

Figure 8: Power law model for the creep data in Figure 7 with $\overline{m} = 0.264$ ($T_r = 115^oC, t_{er} = 879\ hr$).

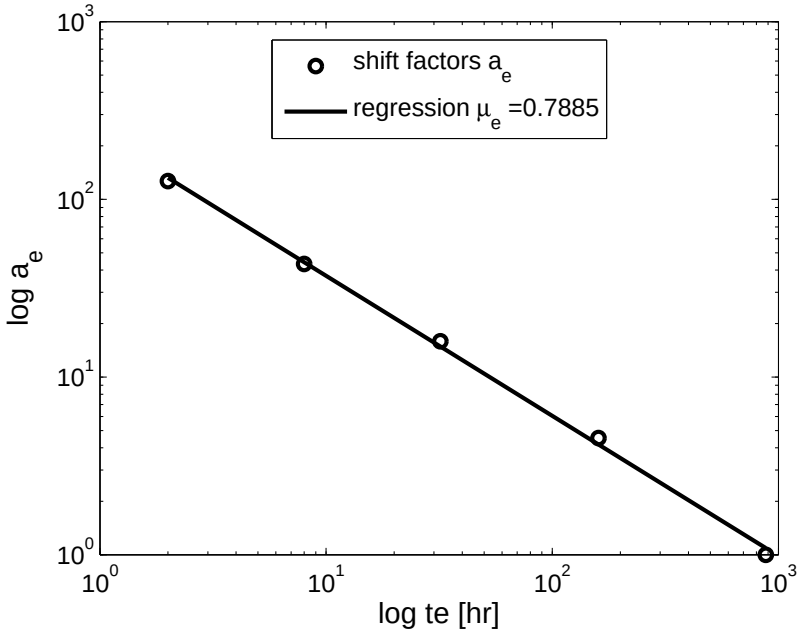

Figure 9: Ageing shift factor plot for the creep data in Figure 8. The data point on the lower right corner of the figure is the shift factor $a_e = 1$ at $t_{er} = 879\,hr$ $(T_r = 115^oC)$.

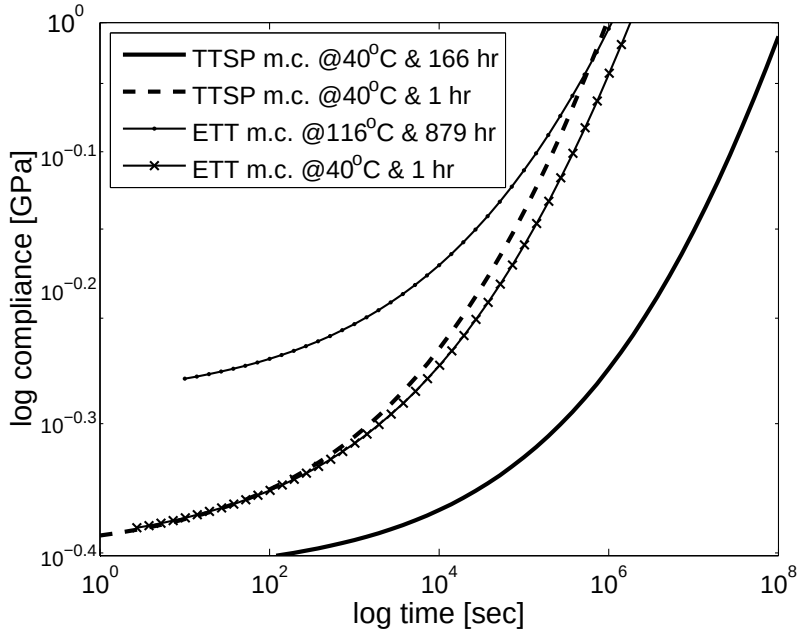

Figure 10: Comparison between momentary master curves obtained from temperature and ageing study. The original momentary master curves have been shifted to a common temperature $T = 60^oC$ and age $t_e = 1\ hr$.

$T[^oC]$	D_0	D_1	m	$\log a_T$	$\log b_T$
40	0.36	0.016	0.166	1	1
60	0.396	0.008	0.227	1.742	1.051
80	0.429	0.004	0.306	4.033	1.103
90	0.438	0.009	0.264	7.758	1.147
115	0.518	0.016	0.271	67.114	1.35
120	0.588	0.02	0.294	229.328	1.496
Average	0.455	0.012	0.255	-	-
COV	0.184	0.496	0.201	-	-

Table 1: Regression parameters and shift factors for the TTSP study depicted in Figure 3.

Age t_e	D_0	D_1	m
879	0.503	0.018	0.239
160	0.523	0.014	0.287
32	0.511	0.026	0.262
8	0.536	0.032	0.269
2	0.58	0.018	0.364
Average	0.518	0.022	0.264
COV	0.028	0.361	0.075

Table 2: Initial regression parameters for the ageing study depicted in Figure 7.

Age t_e	D_0	D_1	m	$\log a_e$	b_e
879	0.518	0.012	0.264	0	0
160	0.512	0.018	0.264	0.657	0.006
32	0.513	0.026	0.264	1.201	0.005
8	0.533	0.033	0.264	1.637	-0.015
2	0.53	0.044	0.264	2.102	-0.012
Average	0.521	0.027	0.264	-	-
COV	0.019	0.468	0	-	-

Table 3: Regression parameters and shift factors for the ageing study depicted in Figure 7.

References

[1] E. J. Barbero, Finite Element Analysis of Composite Materials, Taylor & Francis, 2007.

[2] J. G. Creus, Viscoelasticity: Basic Theory and Applications to Concrete Structures, Springer-Verlag, 1986.

[3] L. C. E. Struik, Physical aging in amorphous polymers and other materials, Elsevier Scientific Pub. Co. ; New York, 1978.

[4] J. Sullivan, Creep and physical aging of composites, Composites Science and Technology 39 (3) (1990) 207 – 32.
URL http://dx.doi.org/10.1016/0266-3538(90)90042-4

[5] T. Gates, M. Feldman, Time-dependent behavior of a graphite/thermoplastic composite and the effects of stress and physical aging, Journal of Composites Technology and Research 17 (1) (1995/01/) 33 – 42.

[6] E. J. Barbero, Web resource.
URL http://www.mae.wvu.edu/barbero/

[7] D. Matsumoto, Time-temperature superposition and physical aging in amorphous polymers, Polymer Engineering and Science 28 (20) (1988) 1313 – 1317.

[8] S. Vleeshouwers, A. Jamieson, R. Simha, Effect of physical aging on tensile stress relaxation and tensile creep of cured epon 828/epoxy adhesives in the linear viscoelastic region, Polymer Engineering and Science 29 (10) (1989) 662 – 670.

[9] E. Barbero, K. Ford, Determination of aging shift factor rates for field-processed polymers, Journal of Advanced Materials 38 (2) (2006) 7–13.

[10] R. Bradshaw, L. Brinson, Physical aging in polymers and polymer composites: An analysis and method for time-aging time superposition, Polymer Engineering and Science 37 (1) (1997) 31–44.

[11] A. Lee, G. McKenna, Viscoelastic response of epoxy glasses subjected to different thermal treatments, Polymer Engineering and Science 30 (7) (1990) 431 – 5.

[12] A. Lee, G. B. McKenna, Physical ageing response of an epoxy glass subjected to large stresses, Polymer 31 (3) (1990) 423 – 430.
URL http://dx.doi.org/10.1016/0032-3861(90)90379-D

[13] E. J. Barbero, M. J. Julius, Time-temperature-age viscoelastic behavior of commercial polymer blends and felt filled polymers, Mechanics of Advanced Materials and Structures 11 (3) (2004) 287–300.

[14] E. Barbero, K. Ford, Equivalent time temperature model for physical aging and temperature effects on polymer creep and relaxation, ASME Journal of Engineering Materials and Technology 126 (4) (2004) 413–419.

[15] E. Barbero, S. Rangarajan, Long-term testing of trenchless pipe liners, Journal of Testing and Evaluation 33 (6) (2005) 377–384.

[16] E. Barbero, R. Luciano, Micromechanical formulas for the relaxation tensor of linear viscoelastic composites with transversely isotropic fibers, International Journal of Solids and Structures 32 (13) (1995) 1859–1872.

[17] R. Luciano, E. J. Barbero, Analytical expressions for the relaxation moduli of linear viscoelastic composites with periodic microstructure, ASME J Appl Mech 62 (3) (1995) 786–793.